



CHORUS

This is the accepted manuscript made available via CHORUS. The article has been published as:

High-Temperature Quantum Anomalous Hall Effect in n-p Codoped Topological Insulators

Shifei Qi, Zhenhua Qiao, Xinzhou Deng, Ekin D. Cubuk, Hua Chen, Wenguang Zhu, Efthimios Kaxiras, S. B. Zhang, Xiaohong Xu, and Zhenyu Zhang

Phys. Rev. Lett. **117**, 056804 — Published 27 July 2016

DOI: [10.1103/PhysRevLett.117.056804](https://doi.org/10.1103/PhysRevLett.117.056804)

High-Temperature Quantum Anomalous Hall Effect in n - p Codoped Topological Insulators

Shifei Qi,^{1,2} Zhenhua Qiao,^{1,3} Xinzhou Deng,^{1,3} Ekin D. Cubuk,⁴ Hua Chen,⁵ Wenguang Zhu,^{1,3} Efthimios Kaxiras,⁴ S. B. Zhang,⁶ Xiaohong Xu,^{2,*} and Zhenyu Zhang^{1,†}

¹*International Center for Quantum Design of Functional Materials,
Hefei National Laboratory for Physical Sciences at Microscale,
and Synergetic Innovation Center of Quantum Information and Quantum Physics,
University of Science and Technology of China, Hefei, Anhui 230026, China*

²*School of Chemistry and Materials Science, Shanxi Normal University, Linfen, Shanxi 041004, China*

³*Department of Physics, University of Science and Technology of China, Hefei, Anhui 230026, China.*

⁴*School of Engineering and Applied Sciences, Harvard University, Cambridge, Massachusetts 02138, USA*

⁵*Department of Physics, The University of Texas at Austin, Austin, Texas 78712, USA*

⁶*Department of Physics, Applied Physics and Astronomy,
Rensselaer Polytechnic Institute, Troy, New York 12180-3590, USA*

(Dated: June 29, 2016)

The quantum anomalous Hall effect (QAHE) is a fundamental quantum transport phenomenon that manifests as a quantized transverse conductance in response to a longitudinally applied electric field in the absence of an external magnetic field, and promises to have immense application potentials in future dissipation-less quantum electronics. Here we present a novel kinetic pathway to realize the QAHE at high temperatures by n - p codoping of three-dimensional topological insulators. We provide proof-of-principle numerical demonstration of this approach using vanadium-iodine (V-I) codoped Sb_2Te_3 and demonstrate that, strikingly, even at low concentrations of $\sim 2\%$ V and $\sim 1\%$ I, the system exhibits a quantized Hall conductance, the tell-tale hallmark of QAHE, at temperatures of at least ~ 50 Kelvin, which is three orders of magnitude higher than the typical temperatures at which it has been realized so far. The underlying physical factor enabling this dramatic improvement is tied to the largely preserved intrinsic band gap of the host system upon compensated n - p codoping. The proposed approach is conceptually general and may shed new light in experimental realization of high-temperature QAHE.

PACS numbers: 73.20.At; 74.43.Cd; 75.70.Tj.

Two-dimensional electron systems (2DESs) may exhibit a variety of novel quantum phenomena. One prominent example is the quantum Hall effect (QHE) [1, 2]. The underlying mechanisms are the formation of insulating bulk and gapless chiral edge states (Fig. 1a). The chiral transport property protects the edge states to be robust against impurity scattering [3, 4]. This essentially renders the sample edges to act as perfect one-dimensional conducting wires, which are of great interest as potential building blocks in dissipation-less electronics, such as interconnects between chips. However, a major constraint for practical use is the requirement of strong magnetic fields, which is impractical for realistic applications. Realizing quantum anomalous Hall effect (QAHE) would circumvent this problem because it manifests the same hallmark features as the QHE but does not require external magnetic fields [5]. The QAHE originates from an intricate cooperation between the intrinsic magnetism and spin-orbit coupling. The initial proposal for realizing the QAHE was based on a honeycomb lattice model [5]. Since then, especially after the experimental discoveries of graphene [6] and topological insulators (TIs) [7, 8], much effort has been made to exploring new platforms for realizing the QAHE in these and related systems [9–20]. TIs are superior to graphene for this purpose because

of their inherently strong spin-orbit coupling, which narrows the search for suitable materials to those harboring intrinsic magnetism. One possible way to induce magnetism in TIs is to dope magnetic elements [12, 21–24]. This approach has indeed led to the first experimental realizations of QAHE in Cr/V-doped $(\text{Bi,Sb})_2\text{Te}_3$ thin films [25–28].

So far, all the experimentally observed QAHEs were achieved at extremely low temperatures, typically ~ 30 mK, making drastically increasing the QAHE observation temperature a daunting challenge both fundamentally and for potential applications. In general, there are two crucial energy scales, the actual band gap of the magnetic TI thin films and the ferromagnetic Curie temperature, with the smaller of the two defining the upper limit of the QAHE observation temperature. In earlier theoretical studies of the QAHE, a rigorous analysis of the delicate interplay between these two energy scales has been lacking, at least not at the materials-specific first-principles level. For example, in the pioneering work predicting the QAHE in magnetic TIs [12], the estimated Curie temperature is high, but neither the bulk nor the thin film band gap was obtained from first-principles calculations, making it impossible to critically assess the likely QAHE observation temperature. More

recent studies have shown that, in single-element doping, the bulk gap decreases with the increase of doping concentration due to introducing impurity states into the bulk gap [29]. Furthermore, spatial inhomogeneity of magnetic dopants is unavoidable, which further decreases the bulk gap. Therefore, how to preserve the intrinsic gap in the presence of magnetic dopants as large as possible is the central issue in exploring high-temperature QAHE.

In this Letter, we propose a versatile approach to realize high-temperature QAHE by using compensated n - p codoping to establish high-temperature ferromagnetism in 3D-TIs. This approach in large part does not alter the bulk gaps and thus addresses the primary challenge that has hindered experimental realization of high-temperature QAHE in TIs [25–28]. We provide numerical proof-of-principle demonstration of this approach using a prototypical example, by codoping Sb_2Te_3 with p -type vanadium (V) and n -type iodine (I). These dopants are chosen because of their preference to form n - p pairs due to mutual electrostatic attraction, thereby enhancing their solubility. More importantly, we show that whereas doping with V alone would undesirably shift the Fermi level into the valence band and shrink the bulk gap, codoping with I recovers the insulating nature while also significantly restores the intrinsic bulk gap of the TI. Moreover, for all the codoping concentrations considered, the coupling between the hard magnetic V dopants always gives a stable ferromagnetic order. Strikingly, even at a low codoping concentration of 2.08% V and 1.39% I (which amounts to compensated one-to-one V-I codoping), an estimated Curie temperature about 49 Kelvin can be reached. Aside from the bulk properties, the band gaps associated with the surface states of corresponding thin film structures can also be as large as 53 meV, much larger than what is needed to sustain ferromagnetism at the high Curie temperatures. Explicit calculations of Berry curvatures further confirm that the V-I codoped Sb_2Te_3 thin films can harbor QAHE with quantized Hall conductance of $\sigma_{xy} = e^2/h$. The proposed approach thus offers a versatile route to realize high-temperature QAHE in different TIs and related materials.

Our first-principles calculations were performed using the projected augmented-wave method [30] as implemented in the Vienna Ab-initio Simulation Package (VASP) [31]. The generalized gradient approximation (GGA) of Perdew-Burke-Ernzerhof (PBE) type was used to treat the exchange-correlation interaction [32]. A $4 \times 4 \times 1$ Sb_2Te_3 supercell is chosen to study the magnetic coupling between V dopants. Each supercell comprises three quintuple layers (QLs), including 96 Sb atoms and 144 Te atoms. For thin film calculations, the thickness was chosen to be six QLs, including 192 Sb and 288 Te atoms. A vacuum buffer space of 30 Å was used to prevent coupling between adjacent slabs. The kinetic energy cutoff was set to 250 eV. During structural relaxation, all atoms were allowed to relax until the Hellmann-

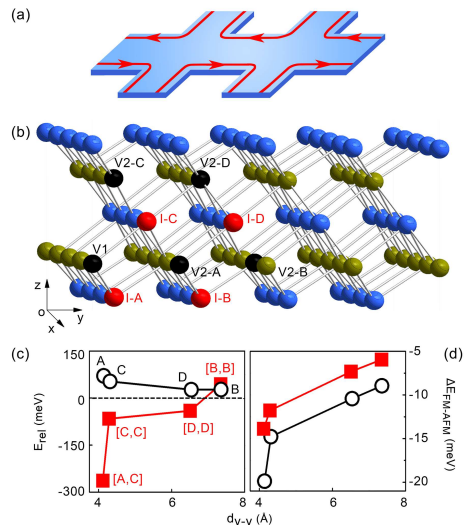


FIG. 1: (a) Schematic of a Hall-bar device with chirally propagating edge modes. (b) The $4 \times 4 \times 1$ supercell of Sb_2Te_3 with only one of three QLs shown for clarity. The notations are: V1 is the site, where one V atom substitutes one Sb atom; V2-A - V2-D are sites that can be occupied by a second V dopant; I-A - I-D designate sites that can be occupied by one I dopant. (c) V-V interaction energy E_{rel} vs. the V-V separation $d_{\text{V-V}}$ of V doped (open black circles) and V-I codoped Sb_2Te_3 (filled red squares), respectively. For the V doped case, the label of each open circle indicates the position of the second V atom. In the V-I codoped case, one I is fixed at I-A, and the two labels in each square bracket denote the positions of the second V and second I, respectively. (d) Magnetic coupling between two V dopants vs. $d_{\text{V-V}}$ of V doped (open black circles) and V-I codoped (filled red squares) Sb_2Te_3 , respectively.

Feynman force on each atom is smaller than $0.01 \text{ eV}/\text{Å}$. The Brillouin-zone integration was carried out by respectively using $3 \times 3 \times 2$ and 1×1 Monkhorst-Pack grids for bulk and thin film systems. Unless mentioned otherwise, spin-orbit coupling was considered in all calculations, and the GGA+U method was used with on-site repulsion parameter $U=3.00 \text{ eV}$ [33] and exchange parameter $J=0.87 \text{ eV}$, where U is applied to the more localized $3d$ -orbitals of V dopants. The Curie temperature T_C was estimated within the mean-field approximation $k_B T_C = \frac{2}{3} x \sum_{i \neq 0} J_{0i}$ [34], where x is the dopant concentration, and J_{0i} is the on-site exchange parameter.

To elucidate the role of codoping in realizing high-temperature QAHE, we first investigate the energetics and magnetic behavior of Sb_2Te_3 solely doped with V, whereby V dopants substitute Sb atoms [35]. The interaction energy between two V atoms is defined as

$$E_{\text{rel}} = E_{2\text{V}} + E_{0\text{V}} - 2E_{1\text{V}}, \quad (1)$$

where $E_{i\text{V}}$ is the total energy of the Sb_2Te_3 systems containing i ($i=0, 1, 2$) V atoms. We found that the V-V interaction is repulsive (Fig. 1c). Thus the energetics

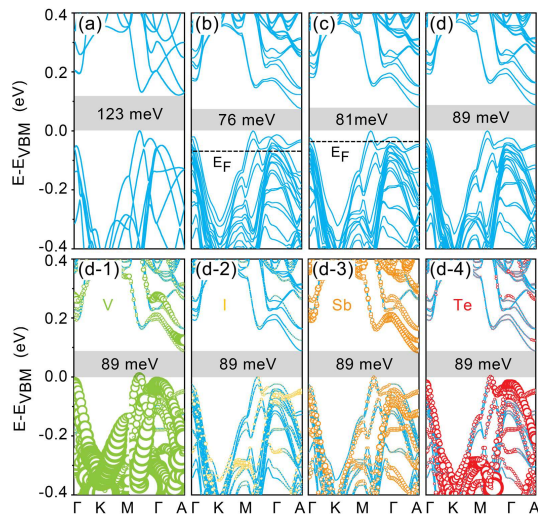


FIG. 2: Band structures of V doped and V-I codoped Sb_2Te_3 . (a) Pure Sb_2Te_3 with a bulk band gap of 123 meV; (b) For 2.08% V doping, the Fermi level shifts into the valence band, and the bulk gap decreases to 76 meV; (c) Additional 0.69% I codoping slightly moves the Fermi level towards the bulk gap and enlarges the gap to 81 meV; (d) A further increase of I codoping to 1.39% compensates the V dopants and shifts the Fermi level into the bulk gap of 89 meV, effectively recovering the insulating nature of the system. (d-1)-(d-4) Different characters of the bands shown in panel (d), obtained by projecting the Kohn-Sham states onto the local orbitals of a single atom for each element.

dictate that the V dopants arrange according to a diluted distribution. We also found that the V-V magnetic coupling is ferromagnetic for all the V-V separation considered, strongly indicating a preponderance toward a diluted ferromagnetism (Fig. 1d) - the magnetic coupling is defined as the energy difference between ferromagnetic and anti-ferromagnetic configurations.

One important finding from our comparison of the electronic band structures of pristine (Fig. 2a) and V-doped Sb_2Te_3 (Fig. 2b) is that solely doping with V drives the system from an insulator (Fig. 2a) to a heavily p -doped metal (Fig. 2b), even at a low concentration of 2.08%, which is consistent with previous experimental findings [35]. V doping also decreases the bulk gap from 123 to 76 meV at the 2.08% V concentration, which originates from the V contribution to the valence band maximum (VBM) (Fig. 2(d-1)) [36]. Consequently, V doping alone cannot convert Sb_2Te_3 into a magnetic TI.

We now demonstrate that to recover the insulating nature of Sb_2Te_3 it is necessary to compensate the extra charge introduced by V dopants, by adding an additional type of dopant with opposite charge, i.e., in this case an n -type dopant. We chose I as the dopant to substitute Te in Sb_2Te_3 , which results in an n -type doping. This choice was inspired by the fact that SbTeI and BiTeI are naturally existing materials [37]. Moreover,

I possesses larger spin-orbit coupling than Te, which is likely to have the added benefit for enhancing the topological phases [38, 39]. Using an n - p codoping approach has also the added benefits of stabilizing the constituent dopants (because of their mutual electrostatic attraction), increasing their solubility, and potentially leading to a higher magnetic transition temperature, as in the case of diluted magnetic semiconductors [40]. Additionally, we note that the experimentally fabricated Sb_2Te_3 is usually a light-doped TI (therefore a conductor) due to the defects, which, based on our compensation principle, can be potentially tuned to be an insulator by properly adjusting the ratio of n - and p -doping.

Codoping Sb_2Te_3 with V and I results in striking changes in the band structure. First, codoping with 0.69% I, in addition to 2.08% V doping, shifts the Fermi level upwards (Fig. 2c). For this low I-doping concentration, the system is still a p -doped metal. When the I concentration further increases to 1.39% (which entails one-to-one V-I codoping), the system recovers its insulating phase, and the bulk gap also increases to 89 meV (Fig. 2d). Further analysis of the characters of different elements in the electronic band structure by projecting the Kohn-Sham states onto local orbitals of a *single* atom for each element (Figs. 2d(1)-2d(4)) reveals that the valence band close to the Fermi level is mainly dominated by V, Sb, and Te atoms, while I contributes mainly to the lower part of valence bands. These results directly reflect the strong bonding interaction between I and the surrounding V/Sb atoms, because I has larger electronegativity than Te, and the resulting large energy difference between bonding and anti-bonding orbitals helps to enlarge the bulk gap. Therefore, the introduction of I not only shifts the Fermi level into the bulk gap but also enlarges the gap size, which are the salient features of the compensated n - p codoping scheme. Taken together, these results demonstrate that it is possible to preserve an insulating bulk Sb_2Te_3 even in the presence of doping, provided that one-to-one compensated V-I codoping is used.

Preserving the insulating phase during doping is one key requirement for realizing high-temperature QAHE. The second requirement is to achieve a strong ferromagnetism. We therefore examine the magnetic properties of the V-I codoped system. Before doing so, it is important to investigate how two separate V-I pairs interact in the host system. Our calculations show, first, that the pair-pair interaction is attractive (Fig. 1c). A second conclusion is that the magnetic coupling between two magnetic moments associated with V dopants is ferromagnetic, with $\Delta E_{\text{FM-AFM}} < 0$, for all the considered dopant separation ranges. In addition, we found that, when compared to the pure V-doped case, the resultant magnetic moment of a V-I pair is larger, but the coupling strength between two such pairs is somewhat smaller. This can be attributed to the fact that the V-I codoped

system becomes insulating, whereas the V-doped system is metallic and has delocalized charge carriers that mediate stronger magnetic coupling. Taken together, these findings indicate that the n - p codoping scheme efficiently leads to a stable ferromagnetic state even at relatively low codoping concentrations, which is highly advantageous compared to other approaches that rely on heavy magnetic doping [25–27].

The ferromagnetism induced using our codoping scheme is highly robust and has the potential to exist at high temperatures. For the particular doping concentrations, using the magnetic coupling strengths extracted from our first-principles calculations, we estimate the Curie temperature within mean-field theory [34] to be $T_C = 49$ (152) Kelvin for codoping concentration of 2.08% V and 1.39% I [the results were obtained within GGA+U (GGA) by placing two V-I pairs in diluted configuration at one QL]. In Supplemental Material, we also provide the estimated Curie temperature from Monte Carlo Simulations. With further increase of the codoping concentration it is possible to raise the Curie temperature, as long as the dopant pair concentrations are still low enough to be away from potential dopants' clustering [41]. Therefore, the present estimations give a lower limit on the Curie temperature at such a low codoping concentration.

Our proof-of-principle demonstration thus shows that V-I codoped Sb_2Te_3 is a ferromagnetic insulator with a sizable gap, making the system a highly desirable candidate for realizing high-temperature QAHE. As a generic guiding principle, we expect that magnetic TIs with large bulk band gaps also likely exhibit sizable band gaps in thin-film geometry. This expectation is confirmed by our detailed quantitative calculations. To demonstrate that such systems can indeed harbor QAHE for a wide range of codoping concentrations, we have calculated and analyzed the band structures of intrinsic and V-I codoped Sb_2Te_3 thin films and shown that these systems yield the quantized Hall conductance $\sigma_{xy} = e^2/h$ expected for the QAHE. To that end, first, we have shown that these codoped systems harbor large energy gaps around the Dirac point. In the absence of dopants, the surface of a Sb_2Te_3 thin film hosts a massless Dirac fermion, manifested as the trademark linear Dirac dispersion near the gamma point [42] (Fig. 3a). After introducing magnetic dopants, the Dirac fermion acquires a finite mass due to the presence of the intrinsic ferromagnetism, which in principle can lead to the QAHE [8]. Here we show the calculated band structures and Berry curvatures, along the high-symmetry directions near the gamma point, for three different codoping concentrations 2.08% V and 1.39% I (Fig. 3b), 4.16% V and 2.78% I (Fig. 3c), and 6.25% V and 4.17% I (Fig. 3d). For all the codoping concentrations the Fermi level lies inside the gap, which is enlarged from 53 (Fig. 3b) to 84 meV (Fig. 3d) when the codoping concentration increases. This proves that

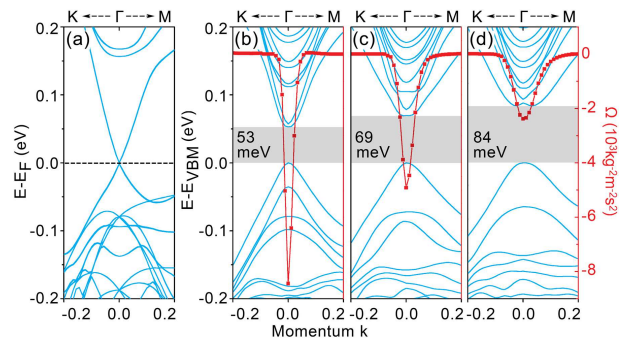


FIG. 3: (a) Band structure of a Sb_2Te_3 thin film calculated in a 4×4 Sb_2Te_3 supercell with a thickness of 6QLs along high symmetry directions. (b)-(d) Solid lines: Band structures of V-I codoped Sb_2Te_3 with the film thickness of 6QLs at different codoping concentrations: (b) 2.08% V and 1.39% I, (c) 4.16% V and 2.78% I, and (d) 6.25% V and 4.17% I. Square symbols: Corresponding Berry curvatures.

the V-I codoping drives the conducting surface into an insulator with an appreciable surface band gap, allowing the formation of high-temperature QAHE.

A separate and unambiguous evidence for the manifestation of QAHE is obtained by integrating the Berry curvature of the occupied valence bands using the expression [43, 44]

$$\Omega(\mathbf{k}) = - \sum_n f_n \sum_{n' \neq n} \frac{2\text{Im}\langle \psi_{n\mathbf{k}} | v_x | \psi_{n'\mathbf{k}} \rangle \langle \psi_{n'\mathbf{k}} | v_y | \psi_{n\mathbf{k}} \rangle}{(E_{n'} - E_n)^2}, \quad (2)$$

where n is the band index, E_n and $\psi_{n\mathbf{k}}$ are the eigenvalue and eigenstate of the band n , $v_x = \partial E / \partial k_x$ and $v_y = \partial E / \partial k_y$ are velocity operators along x and y directions within the film plane, and $f_n = 1$ for all occupied bands. This integration gives the corresponding Hall conductance [44]. The Berry curvature distribution along the high symmetry directions shows a large negative peak near the gamma point and zero elsewhere (Figs. 3(b)-3(d)). As a consequence, the Hall conductance with the Fermi level lying inside the band gap must be nonzero. With the increase of the surface band gap, the region with finite Berry curvatures broadens, and the curvature peak gradually decreases, potentially signifying the unchanged Hall conductance. Our quantitative calculations reveal that the Hall conductance is indeed quantized, i.e. $\sigma_{xy} = e^2/h$, for all the three codoping concentrations, and thus that the system is in a QAHE state.

So far, the QAHE had been experimentally observed by using the host TI $(\text{Bi,Sb})_2\text{Te}_3$ doped with the magnetic element of Cr or V [25–28]. We anticipate that these experiments could be extended to using the proposed codoping approach to realize high-temperature QAHE. As highly related developments, here we mention that the non-compensated version of n - p codoping concept has been successfully exploited to narrow the band gaps of wide band gap semiconductors such as TiO_2 for a broad

range of applications in clean energy [40, 45, 46]. Additionally, one clear advantage of the compensated n - p codoping scheme is that the n - p codopants prefer to be distributed homogeneously, as confirmed in diluted magnetic semiconductors [40, 47].

In conclusion, our findings demonstrate that codoping TIs provides a versatile route to realizing the QAHE at high temperatures [48]. Our proof-of-principle demonstrations revealed that codoping results in: 1) the formation of large band gaps, 2) high Curie temperatures, 3) quantized Hall conductance. These manifestations originate from the realization of hard ferromagnetism (in the present case due to V dopants), strong spin-orbit coupling (here because of the I dopants), and, most crucially, the pinning of the Fermi level inside the largely preserved intrinsic TI bulk gap. Even at very low concentrations, the lower-bound temperature for observing the QAHE in the V-I codoped TI is ~ 50 K, which is three orders of magnitude higher than what was previously reported so far [25–27]. By further increasing and tailoring the codoping and TI environments, it is feasible to further increase the QAHE observation temperature.

We are grateful to the financial support of NSFC (Grant No.: 51025101, 11104173, 11034006, 11474265, and 61434002) and NBRPC (Grant No.: 2014CB921103). Z.Q. also acknowledges support from the China Government Youth 1000-Plan Talent Program. S.B.Z. is supported by the US DOE Office of Basic Energy Sciences (Grant No.: DE-SC0002623). H.C. is supported by NSF (Grant No.: DMR-1122603). The supercomputing center of USTC and the National Energy Research Supercomputer Center of the US Department of Energy are gratefully acknowledged for high performance computing assistance.

S.F. Qi and Z.H. Qiao contributed equally to this work.

* Correspondence author: xuxh@dns.sxnu.edu.cn

† Correspondence author: zhangzy@ustc.edu.cn

- [1] K. Klitzing, G. Dorda, and M. Pepper, *Phys. Rev. Lett.* **45**, 494 (1980).
- [2] R. B. Laughlin, *Phys. Rev. B* **23**, 5632 (1981).
- [3] B. I. Halperin, *Phys. Rev. B* **25**, 2185 (1982).
- [4] A. H. MacDonald and P. Streda, *Phys. Rev. B* **29**, 1616 (1984).
- [5] F. D. M. Haldane, *Phys. Rev. Lett.* **61**, 2015 (1988).
- [6] A. H. Castro Neto, F. Guinea, N. M. R. Peres, K. S. Novoselov, and A. K. Geim, *Rev. Mod. Phys.* **81**, 109-162 (2009).
- [7] M. Z. Hasan and C. L. Kane, *Rev. Mod. Phys.* **82**, 3045-3067 (2010).
- [8] X. L. Qi and S. C. Zhang, *Rev. Mod. Phys.* **83**, 1057-1110 (2011).
- [9] M. Onoda and N. Nagaosa, *Phys. Rev. Lett.* **90**, 206601 (2003).
- [10] C. X. Liu, X. L. Qi, X. Dai, Z. Fang, and S. C. Zhang, *Phys. Rev. Lett.* **101**, 146802 (2008).
- [11] C. Wu, *Phys. Rev. Lett.* **101**, 186807 (2008).
- [12] R. Yu, W. Zhang, H. J. Zhang, S. C. Zhang, X. Dai, and Z. Fang, *Science* **329**, 61-64 (2010).
- [13] Z. H. Qiao, *et al.* *Phys. Rev. B* **82**, 161414(R) (2010).
- [14] Z. F. Wang, Z. Liu, and F. Liu, *Phys. Rev. Lett.* **110**, 196801 (2013).
- [15] K. F. Garrity and D. Vanderbilt, *Phys. Rev. Lett.* **110**, 116802 (2013).
- [16] J. H. Z. Zhu, and R. Wu, *Nano Lett.* **15**, 2074 (2015).
- [17] C. Fang, M. J. Gilbert, and B. A. Bernevig, *Phys. Rev. Lett.* **112**, 046801 (2014).
- [18] J. Wang, B. Lian, H. Zhang, Y. Xu, and S. C. Zhang, *Phys. Rev. Lett.* **111**, 136801 (2013).
- [19] G. F. Zhang, Y. Li, and C. Wu, *Phys. Rev. B* **90**, 075114 (2014).
- [20] H. Z. Lu, A. Zhao, and S. Q. Shen, *Phys. Rev. Lett.* **111**, 146802 (2013).
- [21] Y. S. Hor, *et al.* *Phys. Rev. B* **81**, 195203 (2010).
- [22] C. Niu, *et al.* *Appl. Phys. Lett.* **98**, 252502 (2011).
- [23] P. P. J. Haazen, *et al.* *Appl. Phys. Lett.* **100**, 082404 (2012).
- [24] T. Jungwirth, J. Sinova, J. Masek, J. Kucera and A. H. MacDonald, *Rev. Mod. Phys.* **78**, 809-863 (2006).
- [25] C. Z. Chang, *et al.* *Science* **340**, 167 (2013).
- [26] J. G. Checkelsky, *et al.* *Nat. Phys.* **10**, 731 (2014).
- [27] X. Kou, *et al.* *Phys. Rev. Lett.* **113**, 137201 (2014).
- [28] X.-Z. Chang, W. Zhao, D. Y. Kim, H. Zhang, B. A. Assaf, D. Heiman, S.-C. Zhang, C. Liu, M. H. W. Chan, and J. S. Moodera, *Nat. Mater.* **14**, 473 (2015).
- [29] See Supplemental Material, which includes Refs. [50]-[51].
- [30] P. E. Blöchl, *Phys. Rev. B* **50**, 17953 (1994).
- [31] G. Kresse and J. Furthmüller, *Phys. Rev. B* **54**, 11169 (1996).
- [32] J. P. Perdew, *et al.* *Phys. Rev. B* **46**, 6671 (1992).
- [33] We also found that the increasing of Hubbard U , i.e., $U = 6$ eV, gives very limited difference comparing to band structures with $U = 3$ eV.
- [34] L. Bergqvist, O. Eriksson, J. Kudrnovsky, V. Drchal, A. Bergman, L. Nordstrom, and I. Turek, *Phys. Rev. B* **72**, 195210 (2005).
- [35] J. S. Dyck, P. Hajek, P. Lostak, and C. Uher, *Phys. Rev. B* **65**, 115212 (2002).
- [36] J. M. Zhang, W. G. Zhu, Y. Zhang, D. Xiao, and Y. G. Yao, *Phys. Rev. Lett.* **109**, 266405 (2012).
- [37] I. Lefebvre, *et al.* *Phys. Rev. Lett.* **59**, 2471 (1987).
- [38] M. S. Bahramy, B.-J. Yang, R. Arita, and N. Nagaosa, *Nat. Commun.* **3**, 679 (2012).
- [39] M. S. Bahramy, B.-J. Yang, R. Arita, and N. Nagaosa, *Phys. Rev. Lett.* **108**, 247208 (2012).
- [40] W. G. Zhu, Z. Y. Zhang, and E. Kaxiras, *Phys. Rev. Lett.* **100**, 027205 (2008).
- [41] S. F. Qi, H. Chen, X. H. Xu, and Z. Y. Zhang, *Carbon* **61**, 609 (2013).
- [42] D. Kong, *et al.* *Nat. Nano.* **6**, 705 (2011).
- [43] Y. G. Yao, *et al.* *Phys. Rev. Lett.* **92**, 037204 (2004).
- [44] D. Xiao, M. Chang, and Q. Niu, *Rev. Mod. Phys.* **82**, 1959-2007 (2010).
- [45] W. Zhu, *et al.* *Phys. Rev. Lett.* **103**, 226401 (2009).
- [46] C. P. Cheney, P. Vilmercati, E. W. Martin, M. Chiodi, L. Gavioli, M. Regmi, G. Eres, T. A. Callcott, H. H. Weitering, and N. Mannella, *Phys. Rev. Lett.* **112**, 036404 (2014).

- [47] X. Xu, H. Blythe, M Ziese, *et al.* New J. Phys. **8**, 135 (2006).
- [48] The central idea of the V-I codoping scheme was first presented at the 2014 APS March Meeting [49]. During the finalization of this manuscript, we became aware of a related work realizing the QAHE in V-doped $(\text{Bi,Sb})_2\text{Te}_3$ thin films at a temperature of 25 milli Kelvin [28]. We speculate that the low temperature is likely to be inherently tied to the small band gap in the V-Bi codoped system, in which the carriers contributed by the V and Bi dopants are at best only partially compensated.
- [49] S. Qi, Z. Qiao, H. Chen, X. Xu, and Z. Zhang, Bulletin of the American Physical Society, 2014 March Meeting, http://absimage.aps.org/image/MAR14MWS_MAR14-2013-002269.pdf.
- [50] H. Chen, W. Zhu, E. Kaxiras, and Z. Zhang, Phys. Rev. B **79**, 235202 (2009).
- [51] Q. Y. Wu, Z. G. Chen, R. Wu, G. G. Xu, Z. G. Huang, F. M. Zhang, Y. W. Du, Solid State Commun. **142**, 242 (2007).